Antitumor and apoptosis-inducing effects of α-mangostin extracted from the pericarp of the mangosteen fruit (*Garcinia mangostana* L.) in YD-15 tongue mucoepidermoid carcinoma cells

HAE NIM LEE, HYE YEON JANG, HYEONG JIN KIM, SEONG AH SHIN, GANG SIK CHOO, YOUNG SEOK PARK, SANG KI KIM and JI YOUN JUNG

Department of Companion and Laboratory Animal Science, Kongju National University, Yesan-eup, Yesan-gun, Chungnam 340-702, Republic of Korea

Received April 8, 2015; Accepted February 26, 2016

DOI: 10.3892/ijmm.2016.2517

Abstract. α-mangostin is a dietary xanthone which has been shown to have antioxidant, anti-allergic, antiviral, antibacterial, anti-inflammatory and anticancer effects in various types of human cancer cells. In the present study, we aimed to elucidate the molecular mechanisms responsible for the apoptosis-inducing effects of α-mangostin on YD-15 tongue mucoepidermoid carcinoma cells. The results from MTT assays revealed that cell proliferation significantly decreased in a dose-dependent manner in the cells treated with α-mangostin. DAPI staining illustrated that chromatin condensation in the cells treated with 15 μM α-mangostin was far greater than that in the untreated cells. Flow cytometric analysis indicated that α-mangostin suppressed YD-15 cell viability by inducing apoptosis and promoting cell cycle arrest in the sub-G1 phase. Western blot analysis of various signaling molecules revealed that α-mangostin targeted the extracellular signal-regulated kinase 1/2 (ERK1/2) and p38 mitogen-activated protein kinase (MAPK) signaling pathways through the inhibition of ERK1/2 and p38 phosphorylation in a dose-dependent manner. α-mangostin also increased the levels of Bax (pro-apoptotic), cleaved caspase-3, cleaved caspase-9 and cleaved-poly(ADP-ribose) polymerase (PARP), whereas the levels of the anti-apoptotic factors, Bcl-2 and c-myc, decreased in a dose-dependent manner. The anticancer effects of α-mangostin were also investigated in a tumor xenograft mouse model. The α-mangostin-treated nude mice bearing YD-15 tumor xenografts exhibited a significantly reduced tumor volume and tumor weight due to the potent promoting effects of α-mangostin on cancer cell apoptosis, as determined by TUNEL assay. Immunohistochemical analysis revealed that the level of cleaved caspase-3 increased, whereas the Ki-67, p-ERK1/2 and p-p38 levels decreased in the α-mangostin-treated mice. Taken together, the findings of our study indicate that α-mangostin induces the apoptosis of YD-15 tongue carcinoma cells through the ERK1/2 and p38 MAPK signaling pathways.

Correspondence to: Professor Ji Youn Jung, Department of Companion and Laboratory Animal Science, Kongju National University, 54 Daehak-ro, Yesan-eup, Yesan-gun, Chungnam 340-702, Republic of Korea
E-mail: wangza@kongju.ac.kr

Key words: xanthone, α-mangostin, tongue cancer cell, apoptosis, anticancer

Introduction

Cancer is one of the most life-threatening diseases worldwide, and the incidence and mortality of cancer in Korea have continuously increased due to various acquired risk factors, including a Western diet and environmental factors (1). Oral cancer accounts for approximately 3-5% of all cancer cases (2,3); however, unlike cancers in other parts of the body, damage to the facial region can cause psychological disorders in patients and negatively affect their daily life, particularly in terms of eating or speaking. Thus, there is great interest in exploring treatments for oral cancer (4). Oral cancer poses a risk of invasion to adjacent organs and a higher possibility of metastatic relapse. Thus, surgical therapy, radiation and medication in combination are usually used to treat oral cancer; however, severe adverse effects and low treatment efficacy, as well as the ineffective inhibition of cancer cell growth and micrometastasis, results in patients with oral cancer tending to have a poor prognosis (5). It is therefore necessary to find naturally-derived substances to serve as anticancer drugs that are capable of specifically targeting cancer cells, with limited side-effects and potent anticancer effects.

Mangosteen (*Garcinia mangostana* L.) is well known as the 'queen of tropical fruit' due to its delicious taste, and has long been used for medicinal purposes, particularly for the treatment of dermatitis, ulcers and diarrhea, in parts of SoutheastEastern South Asia such as Malaysia, Indonesia, Taiwan, Philippines, India and Sri Lanka (6). It has been reported that xanthone, a component contained within the pericarp (rind or peel) of the mangosteen fruit, has been shown to exert various biological effects, including antioxidant (7), anticancer (8), antibacterial (9,10), anti-inflammatory (11), anti-allergic and antiviral effects (12). Xanthone has also been widely used as an inhibitor of enzymes involved in the oxidation of low-density

lipoprotein (LDL) cholesterol (13), as well as those associated with infections, such as prostaglandin E_2 (PGE_2) and cyclooxygenase-2 (COX-2) (14). Thus far, various xanthones have been found in fruit, fruit skin, tree bark, moss and mold, and approximately 40 different xanthones have been found in the mangosteen fruit (15).

α-mangostin is a key, physiologically active substance contained within the fruit skin of mangosteens that has been demonstrated to inhibit the cell cycle and induce the apoptosis of various cancer cell lines, including colorectal, mammary, liver and prostate cancer cells (8,16-19). In particular, the anticancer effects and the inhibitory effects on lymph node metastasis of α-mangostin have been reported using tumor xenograft mouse models of mammary cancer (19).

The mitogen-activated protein kinase (MAPK) cascade, a pathway used to send external signals to internal cells, is involved in various processes, including cell proliferation and fragmentation, apoptosis and survival. There are also subgroups of MAPKs, which include extracellular signal-regulated kinase (ERK), p38 kinase, and c-jun N-terminal kinase/stress-activated protein kinase (JNK/SAPK). Each group is controlled by its own pathway and performs distinct functions. ERK is mainly involved in cell survival, whereas SAPK and p38 kinase mainly regulate apoptosis (20).

However, the anticancer effects of α-mangostin on oral cancer remain unknown. Thus, in this study, we aimed to investigate the anticancer effects of α-mangostin on oral (tongue) cancer, which is a type of cancer with severe adverse effects and lower treatment efficacy compared with other types of cancer. The naturally-derived substance, α-mangostin, was evaluated in YD-15 cells, a tongue mucoepidermoid carcinoma cell line, in order to examine its inhibitory effects on cancer progression in terms of apoptosis. Accordingly, we focused on the ERK1/2 and p38 MAPK signaling pathways in an aim to elucidate the underlying molecular mechanisms.

Materials and methods

Chemicals, drugs and antibodies. α-mangostin (chemical structure shown in Fig. 1) was purchased from Sigma-Aldrich (St. Louis, MO, USA), dissolved in dimethyl sulfoxide (DMSO) and stored at -20˚C. RPMI-1640 medium, penicillin-streptomycin, trypsin-EDTA and fetal bovine serum (FBS) were purchased from HyClone Laboratories, Inc. (Logan, UT, USA). 3-(4,5-Dimethythiazol-2-yl)-2,5-diphenyltetrazolium bromide (MTT) and DMSO were obtained from Sigma-Aldrich. Cell lysis buffer and 4',6-diamidino-2-phenylindole (DAPI) were purchased from Invitrogen Life Technologies (Carlsbad, CA, USA). The fluorescein isothiocyanate (FITC)-conjugated Annexin V Apoptosis Detection kit was purchased from BD Biosciences (San Diego, CA, USA). Anti-β-actin (#4967), anti-Bax (#2772), anti-Bcl-2 (#2876), anti-caspase-3 (#9662), anti-cleaved caspase-3 (#9661), anti-caspase-9 (#9502), anti-poly(ADP-ribose) polymerase (PARP; #9542), anti-ERK1/2 (#9102), anti-phosphorylated (p)-ERK1/2 (#4376), anti-p38 (#9212), anti-p-p38 (#4631), anti-c-myc (#9027), anti-Ki-67 (#9027) and goat anti-rabbit horseradish peroxidase (HRP)-conjugated (#7074) antibodies were purchased from Cell Signaling Technology, Inc. (Beverly, MA, USA). The DeadEnd™ fluorometric terminal deoxynucleotidyl transferase-mediated dUTP nick-end labeling (TUNEL) assay kit was purchased from Promega Corp. (Madison, WI, USA).

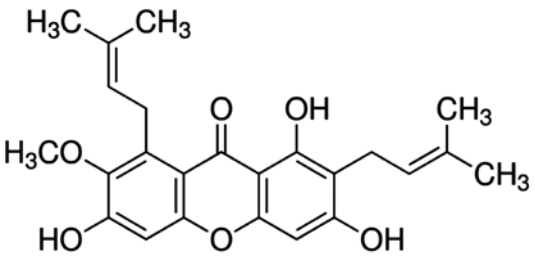

Figure 1. Structure of naturally occurring α-mangostin.

Cell lines and culture. The human tongue mucoepidermoid carcinoma cell line, YD-15, was purchased from the Korean Cell Line Bank (Seoul, Korea) and maintained in RPMI-1640 medium supplemented with 10% FBS and 1% penicillin-streptomycin at 37˚C in a humidified 5% CO_2 atmosphere. The culture medium was replaced every 2-3 days. For α-mangostin treatment, the YD-15 cells were seeded at a density of approximately $3x10^4$ cells/cm^2 in a 175-cm^2 flask and were allowed to adhere overnight.

Cell viability assay. The effects of α-mangostin on YD-15 cell survival were determined by MTT assay. The YD-15 cells were seeded in 96-well plates at a density of $2x10^4$ cells/ml in a volume of 200 μl/well. Following 24 h of incubation, the cells were treated with 10, 15, 20, 25 or 30 μM α-mangostin for 24 h in triplicate. Following treatment, the medium was discarded and 40 μl 5 mg/ml MTT solution were added followed by incubation for an additional 2 h. The medium was then aspirated, and the formazan product generated by the viable cells was solubilized by the addition of 100 μl DMSO. The absorbance of the solutions at 595 nm was determined using a microplate reader (Bio-Rad Laboratories, Inc., Hercules, CA, USA). The percentage of viable cells relative to the untreated (control) cells was estimated.

Nuclear staining. To assess apoptosis, the nuclei of the YD-15 cells were stained with DAPI. The cells were seeded onto 60-mm dishes at a density of $1x10^5$ cells/ml and incubated with 10 or 15 μM α-mangostin for 24 h. Following treatment, the cells were fixed in phosphate-buffered saline (PBS) containing 4% paraformaldehyde for 15 min in an incubator. Following fixation, the cells were washed twice with PBS and the cell nuclei were stained with DAPI in PBS. Fluorescence signals were visualized using a fluorescence microscope (BX41; Olympus Co., Tokyo, Japan) at x200 magnification.

Annexin V staining for the analysis of apoptosis. The Annexin V/propidium iodide (PI) assay was performed according to the manufacturer's instructions (BD Biosciences). Briefly, the YD-15 cells were treated with or without 10 or 15 μM α-mangostin for 24 h, washed twice with cold PBS, and incubated with fluorescein isothiocyanate (FITC)-conjugated Annexin V and phycoerythrin (PE)-conjugated PI in binding buffer at room temperature for 15 min in the dark. The samples were analyzed using a FACSCalibur™ flow cytometer (BD Biosciences).

Flow cytometric analysis of the cell cycle. Cell cycle progression was assayed by measuring DNA fragmentation with PI staining. The YD-15 cells were treated with or without 10 or 15 μM α-mangostin for 24 h, washed twice with PBS and fixed with 70% ethanol for 30 min. Following fixation, the DNA fragments were stained in PBS containing PI and RNase (Sigma-Aldrich) for 30 min at room temperature. After sorting out the viable cells, the fluorescence intensity was measured using a FACSCalibur™ flow cytometer (BD Biosciences).

Western blot analysis. The cells were grown in culture flasks under the same conditions as described above and treated with 10 or 15 μM α-mangostin for 24 h. The cells were washed with PBS and treated with trypsin-EDTA for 1 min. Cell pellets were obtained by centrifugation, lysed in lysis buffer (Invitrogen Life Technologies) and centrifuged at 13,000 rpm for 5 min at 4˚C to obtain whole-cell lysates. Protein concentrations were determined using a Bradford Protein assay kit (Bio-Rad Laboratories Inc.). The samples were stored at -80˚C. The proteins were resolved by sodium dodecyl sulphate-polyacrylamide gel electrophoresis (SDS-PAGE) and transferred electrophoretically onto nitrocellulose membranes (Bio-Rad Laboratories Inc.). The membranes were blocked with Tris-buffered saline (TBS) containing 5% non-fat dry milk and 0.1% Tween-20 at 4˚C for 2 h. After blocking, the membranes were incubated with anti-β-actin, anti-Bax, anti-Bcl-2, anti-caspase-3, anti-caspase-9, anti-PARP, anti-ERK1/2, anti-p-ERK1/2, anti-p38, anti-p-p38 and anti-c-myc antibodies overnight at 4˚C, with gentle shaking. Following incubation with the primary antibodies, the membranes were incubated with HRP-conjugated goat anti-rabbit IgG secondary antibodies for 2 h at room temperature with gentle shaking. After washing the membranes 3 times for 10 min in TBS containing 0.1% Tween-20, bands were detected using enhanced chemiluminescence (ECL) western blotting detection reagents (Pierce, Rockford, IL, USA) according to the manufacturer's instructions. β-actin was used as a loading control. Band density was measured using the ImageJ software (NIH, Bethesda, MD, USA) program.

Animal experiments. Five-week-old male BALB/c nude (nu/nu) mice were purchased from the animal production company of Orient Bio, Inc. (Gyeonggi-do, Korea) and maintained in a controlled environment at 23±5˚C with 40±10% relative humidity with artificial lighting from 8:00 a.m. to 8:00 p.m. in facilities approved by the Companion and Laboratory Animal Science Department of Kongju National University (Chungnam, Korea). The animals were housed in cages and allowed access to sterilized water and commercial rodent chow (Biopia, Seoul, Korea) *ad libitum*. All animal experiments were performed following the approval of the Institutional Animal Care and Use Committee according to the guidelines of Kongju National University.

Tumor xenografts. The YD-15 cells were maintained in RPMI-1640 supplemented with 10% FBS and 1% penicillin-streptomycin at 3˚C in a humidified 5% CO_2 atmosphere. The YD-15 cells were harvested by exposure to trypsin-EDTA. The cells were then washed twice and resuspended in RPMI-1640 medium. The YD-15 cells were then injected subcutaneously ($1x10^7$ cells/0.2 ml medium/animal) into the left and right flanks of the mice using a 27-gauge needle. When the tumors were palpable, the mice were assigned randomly into 3 groups with 3 mice in each (the vehicle-treated controls, and the groups treated with 10 or 20 mg/kg body weight α-mangostin). The doses of α-mangostin (10 and 20 mg/kg) were selected for the *in vivo* experiments using mice based on the results of a previous study by Akao *et al* (8), in which mice administered >20 mg/kg α-mangostin exhibited a significant increase in natural killer (NK) cell activity. Therefore, we selected 20 mg/kg as the dose for use in the present study, as this is the dose that others have reported has no harmful effect. For administration, α-mangostin was dissolved in 0.1% DMSO and further diluted in PBS before injection. α-mangostin was administered intraperitoneally 5 times per week at a dose of 10 or 20 mg/kg body weight, while the control group mice were administered the vehicle only (DMSO in PBS). Tumor weight and size were monitored twice each week. Tumor size was measured using Vernier calipers (Mitutoyo, Kawasaki, Japan). The mice were sacrificed by ether inhalation at 22 days following treatment and the tumors were excised for the measurement of tumor weight. A portion of the tumor was embedded in paraffin and used for TUNEL assays and immunohistochemical analysis.

TUNEL assay. Apoptotic cell death was quantified using a Promega DeadEnd Colorimetric TUNEL system kit according to the manufacturer's instructions (Promega Corp.). Briefly, the tumor tissues were fixed in 10% formalin overnight and embedded in paraffin. The blocks were then cut into 5-μm-thick slices. The tissue sections attached to microscopic slides were then deparaffinized by immersion in xylene and the slides were then washed with 100% ethanol. The samples were rehydrated by sequential immersion in a graded ethanol series (95, 85, 70 and 50%). The tumor sections were visualized using 3'-diaminobenzidine tetrahydrochloride (DAB) solution, treated with mounting reagent, and observed under a microscope (BX41; Olympus Co.) at x200 magnification.

Immunohistochemical analysis. The tumor sections were deparaffinized with two changes of xylene for 10 min, rehydrated with two changes each of 100 and 95% ethanol for 1 min, and rinsed with tap water for 10 min. The sections were then incubated at 4˚C with anti-cleaved caspase-3, anti-p-ERK1/2, anti-p-p38 and anti-Ki-67 antibodies overnight and incubated for 1 h at room temperature with a HRP-conjugated goat anti-rabbit antibody followed by incubation for 1 h. The tumor sections were visualized using DAB solution, treated with mounting reagent, and observed under a microscope (x200 magnification).

Statistical analysis. The results are all expressed as the means ± standard deviations (SD). Differences between mean values for the individual groups were assessed by one-way analysis of variance (ANOVA) with Dunnett's t-tests. A $P<0.05$ was considered to indicate a statistically significant difference.

Results

Inhibitory effects of α-mangostin on the cell survival rate and morphological changes in YD-15 cells. An MTT assay was conducted to examine the effects of α-mangostin on YD-15 cell viability. The YD-15 cells were treated with 0, 10, 15,

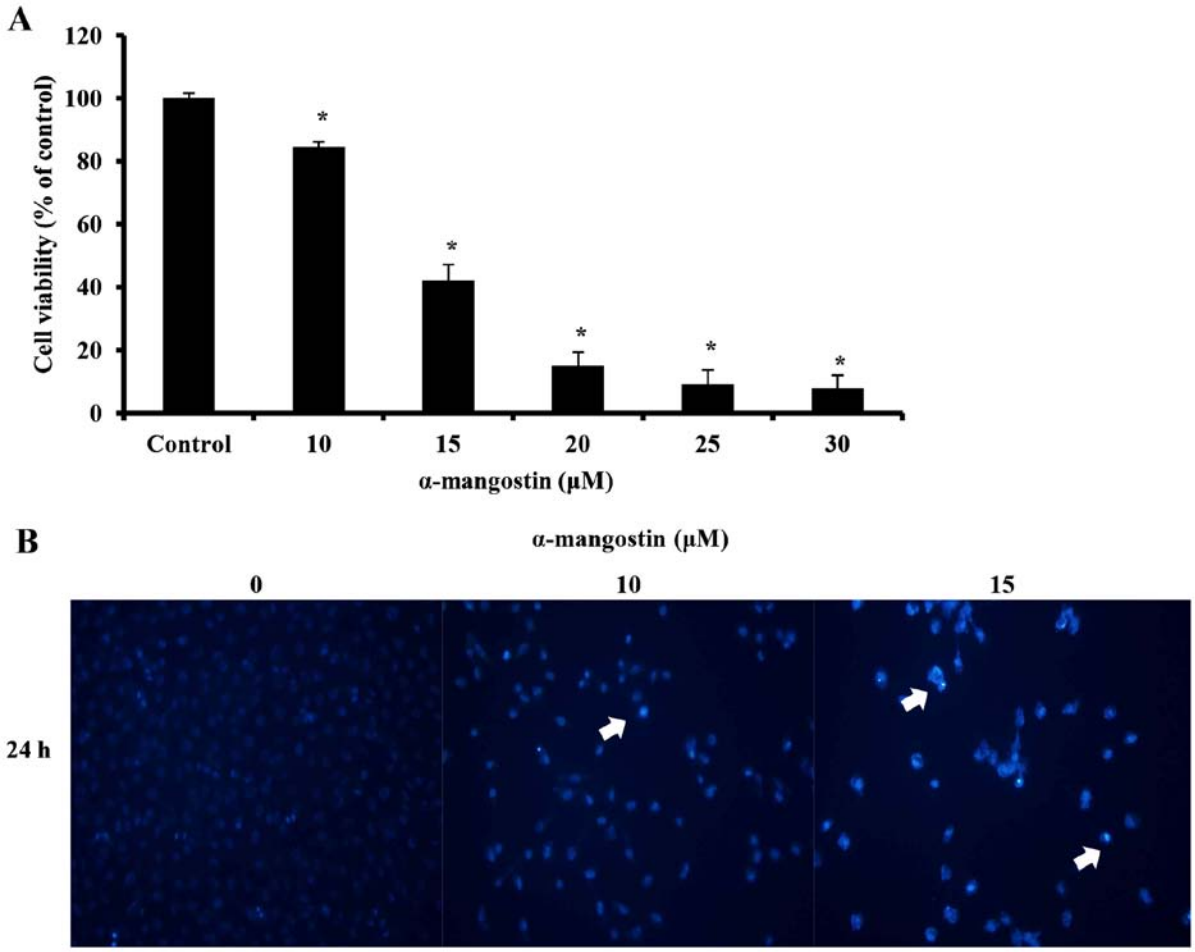

Figure 2. Effects of α-mangostin on cell viability. (A) YD-15 cells were treated with α-mangostin (0, 10, 15, 20, 25 and 30 μM) for 24 h, and cell viability was determined by MTT assay. Results are presented as the means ± standard deviations (SD) of 2 independent experiments each performed in triplicate. Statistical significance was determined by the Dunnett's t-test. *P<0.05, significant difference compared with the untreated controls. (B) DAPI staining. YD-15 cells were treated with α-mangostin (0, 10 and 15 μM) for 24 h. Apoptotic bodies were stained with DAPI. White arrows indicate chromatin condensation in YD-15 cells. Cleaved nuclei were examined by fluorescence microscopy (x200 magnification).

20, 25 and 30 μM α-mangostin for 24 h. Cell viability was inhibited at a concentration of 10 μM (Fig. 2A). Compared with the untreated control cells, the cells treated with 10 μM α-mangostin displayed approximately 15% inhibition, whereas those treated with 15 μM α-mangostin exhibited approximately 58% inhibition. Moreover, the number of viable cells decreased in a concentration-dependent manner. DAPI staining was performed to identify the morphological changes associated with nuclear and chromosomal condensation. The YD-15 cells were treated with 0, 10 and 15 μM α-mangostin for 24 h. DAPI staining was utilized to observe the cells by fluorescence microscopy. As a result, increased apoptosis (indicated by increased chromatin condensation) was observed in the cells treated with 10 and 15 μM α-mangostin compared to the control group (Fig. 2B). These results indicate that α-mangostin decreased the viability of the YD-15 cells, creating apoptotic bodies, thus leading to cellular apoptosis.

Effects of α-mangostin on YD-15 cell apoptosis. Apoptotic cells were analyzed quantitatively by Annexin-V FITC/PI staining to examine the effects of α-mangostin on YD-15 cells. The percentage of apoptotic cells in the untreated (control) group was 16.06% (early apoptotic cells, 4.30%; late apoptotic cells, 11.76%). However, the number of apoptotic cells increased significantly with the increasing concentration of α-mangostin. The percentages of apoptotic cells following treatment with 10 and 15 μM α-mangostin were 28.1 (early apoptotic cells, 10.79%; late apoptotic cells, 17.31%) and 33.65% (early apoptotic cells, 9.84%; late apoptotic cells, 23.81%), respectively (Fig. 3A). Flow cytometry was used to examine the effects of α-mangostin on the YD-15 cell cycle. The percentage of sub-G1 cells in the control group was 0.28% (Fig. 3B). The number of cells in the sub-G1 phase tended to increase in a concentration-dependent manner (10 μM, 1.38% and 15 μM, 6.08%; Fig. 3B). These results suggest that the inhibitory effects of α-mangostin on cell viability are caused by sub-G1 arrest related to apoptosis.

Effects of α-mangostin on the expression of Bcl-2 family proteins. The expression of Bcl-2 family proteins, responsible for controlling apoptosis, was determined by western blot analysis in order to elucidate the mechanisms responsible for the apoptosis induced by α-mangostin in YD-15 cells. The α-mangostin-treated group exhibited an increased expression of the pro-apoptotic factor, Bax, and a decreased expression of the anti-apoptotic factor, Bcl-2, in a concentration-dependent manner (Fig. 4).

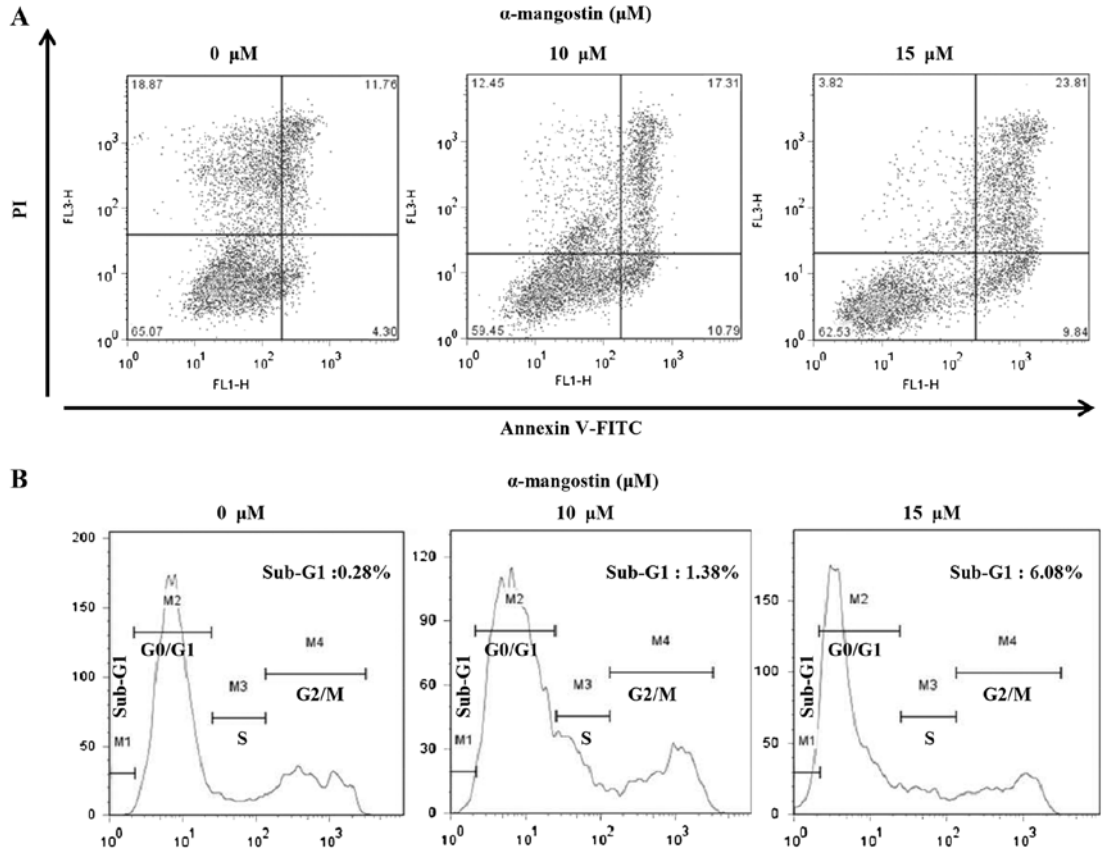

Figure 3. Effects of α-mangostin on apoptosis of YD-15 cells. YD-15 cells were treated with α-mangostin (0, 10 and 15 μM) in complete medium for 24 h. (A) Annexin V/PI staining was performed to detect apoptosis. The lower right quadrant of the fluorescence activated cell sorting (FACS) histogram indicates the percentage of early apoptotic cells (Annexin V-stained cells), while the upper right quadrant indicates the percentage of late apoptotic cells (Annexin V^+/PI-stained cells). (B) The sub-G1 fraction was assessed by PI staining and flow cytometry. Representative staining profiles for 10,000 cells per experiment are shown.

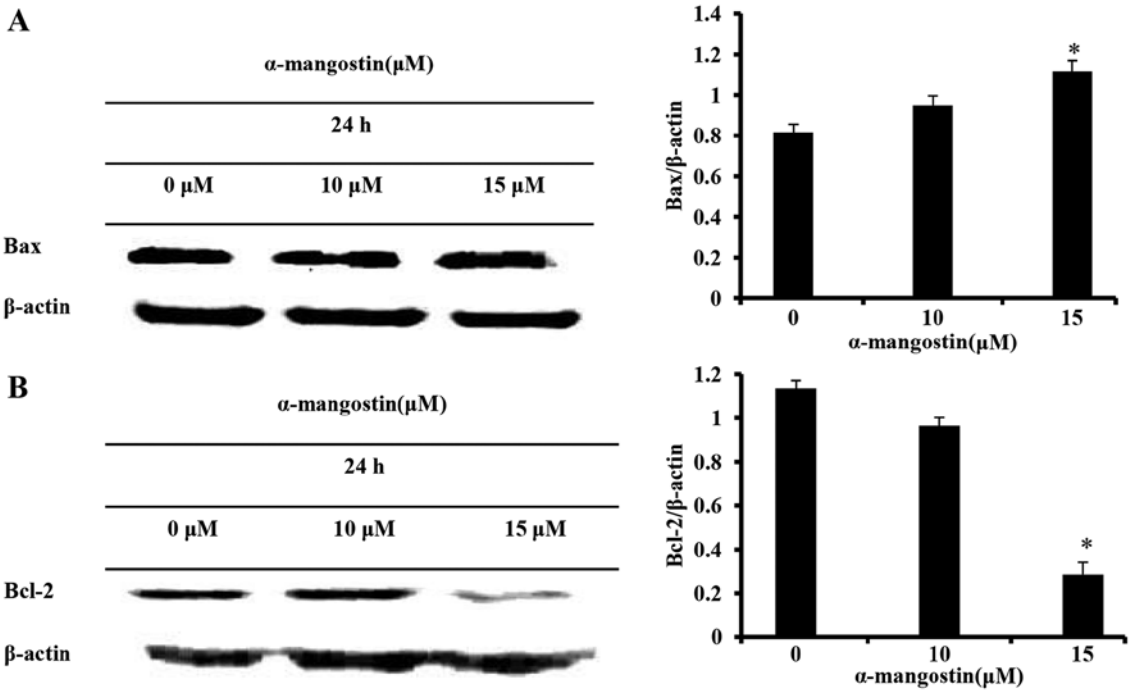

Figure 4. α-mangostin alters the levels of Bax and Bcl-2 in YD-15 cells. YD-15 cells were treated with α-mangostin (0, 10 and 15 μM) for 24 h. Cell lysates were prepared as described in the Materials and methods and analyzed by 12% SDS-PAGE followed by western blot analysis. (A) Membranes incubated with the anti-Bax antibody. (B) Membranes incubated with the anti-Bcl-2 antibody. Blots were also probed with the anti-β-actin antibody to confirm equal sample loading. Data analysis was performed using ImageJ software by measuring the integrated band densities following background subtraction. Each bar represents the means ± SD calculated from 3 independent experiments. Significance was determined by Dunnett's t-test. *P<0.05, significant difference compared to the untreated controls.

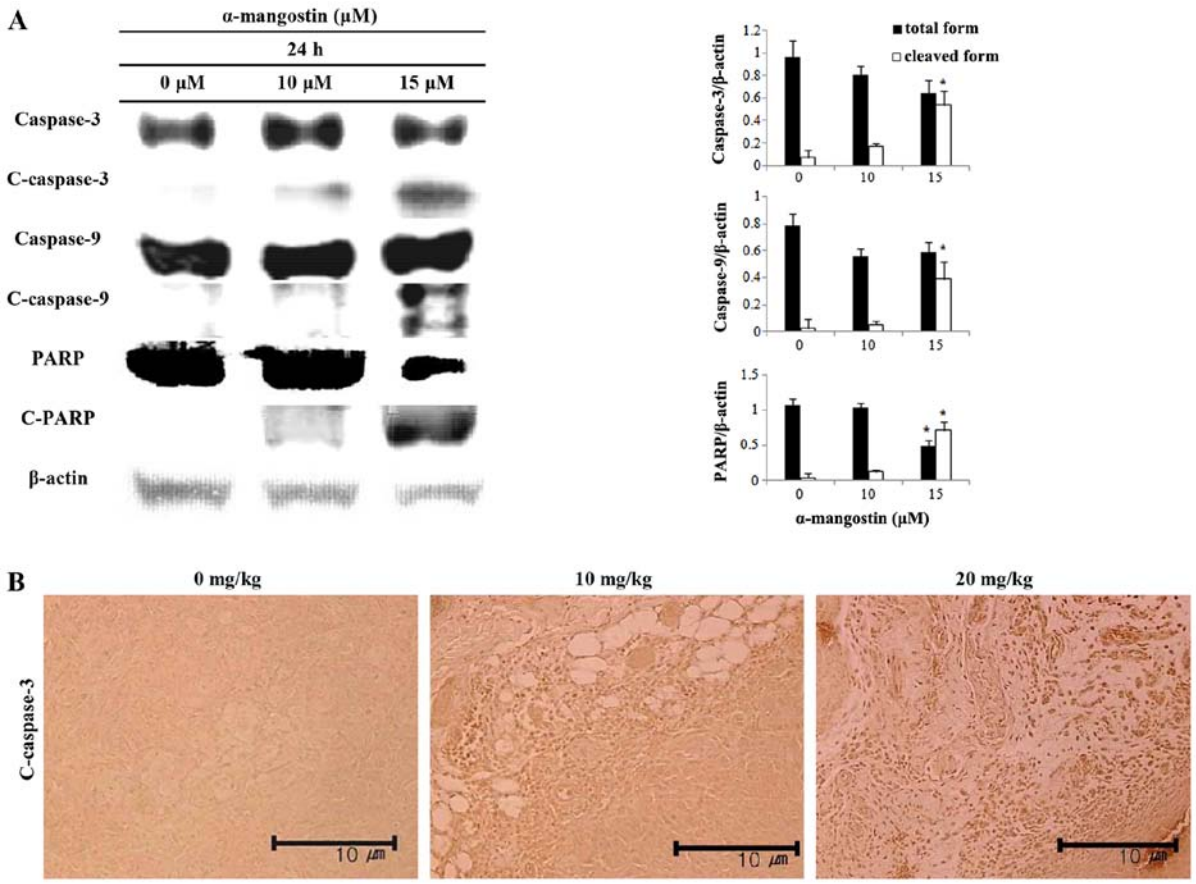

Figure 5. Effects of α-mangostin on apoptosis. (A) YD-15 cells were treated with α-mangostin (0, 10 and 15 μM) for 24 h. Cell lysates were prepared as described in the Material and methods and analyzed by 12% SDS-PAGE, followed by western blot analysis. Membranes were incubated with anti-caspase-3, anti-caspase-9 and anti-PARP antibodies. Blots were also probed with anti-β-actin antibody to confirm equal sample loading. (B) Nude mice were treated with α-mangostin (0, 10 and 20 mg/kg) for 22 days. To identify cleaved (c)-caspase-3 protein, immunohistochemcal staining was performed on tumor tissues collected from mouse xenografts as described in the Material and methods. Cleaved caspase-3 was observed under a microscope and photographed (x200 magnification). Paraffin-embedded tumors were sectioned to 5-μm thickness.

These results imply that the apoptotic mechanism induced by α-mangostin is associated with Bcl-2 family proteins.

Effects of α-mangostin on caspase activation. The expression levels of caspase-3, caspase-9 and PARP were measured by western blot analysis in order to determine the association between the induction of apoptosis by α-mangostin and caspase activation in YD-15 cells. The cells treated with α-mangostin exhibited increased caspase-3 and -9 activity in a concentration-dependent manner (Fig. 5A). The level of cleaved-PARP increased as well. Cleaved caspase-3 was visualized by immunohistochemical analysis in order to examine the effects of α-mangostin on caspase expression in tumor tissues collected from mice with tumor xenografts (Fig. 5B). The tumor tissue from mice treated with α-mangostin exhibited increased levels of cleaved caspase-3 in a concentration-dependent manner, suggesting that the mechanism of apoptosis induced by α-mangostin is related to caspase activation, which in turn induces PARP segmentation.

Effects of α-mangostin on ERK1/2 MAPK and p38 MAPK expression. The levels of ERK1/2, p38 and c-myc were examined by western blot analysis in order to determine whether the induction of apoptosis by α-mangostin involves the MAPK pathway. The inhibition of ERK1/2 and p38 activation, and decreased c-myc expression were observed in the cells treated with α-mangostin in a concentration-dependent manner (Fig. 6A). The levels of p-ERK1/2 and p-p38 were determined by immunohistochemical analysis to determine whether the effects of α-mangostin involve the MAPK pathway in tumor tissue from mice with tumor xenografts (Fig. 6B). The tumor tissue of the mice treated with α-mangostin exhibited decreased levels of p-ERK1/2 and p-p38 in a concentration-dependent manner.

Effects of α-mangostin on mouse tumor xenografts. The effects of α-mangostin on tumor volume in mice with YD-15 tumor xenografts were investigated. α-mangostin was administered by intraperitoneal injection at the dose of 10 mg/kg (low-dose) and 20 mg/kg (high-dose). The mice in the control group received the vehicle (0.5% DMSO in PBS) with the same timing and dosing schedule used for the treatment group. A significant difference in tumor volume emerged in the control group from day 8 onwards following treatment. The mice treated with 20 mg/kg α-mangostin exhibited a tumor volume inhibition rate of 89.9% compared with the control group (Fig. 7A). The sizes of the final tumors in the control and α-mangostin-treated (10 and 20 mg/kg body weight) mice were 639, 105 and 43 mm^3, respectively. Tumor weights in the experimental nude mice were also deter-

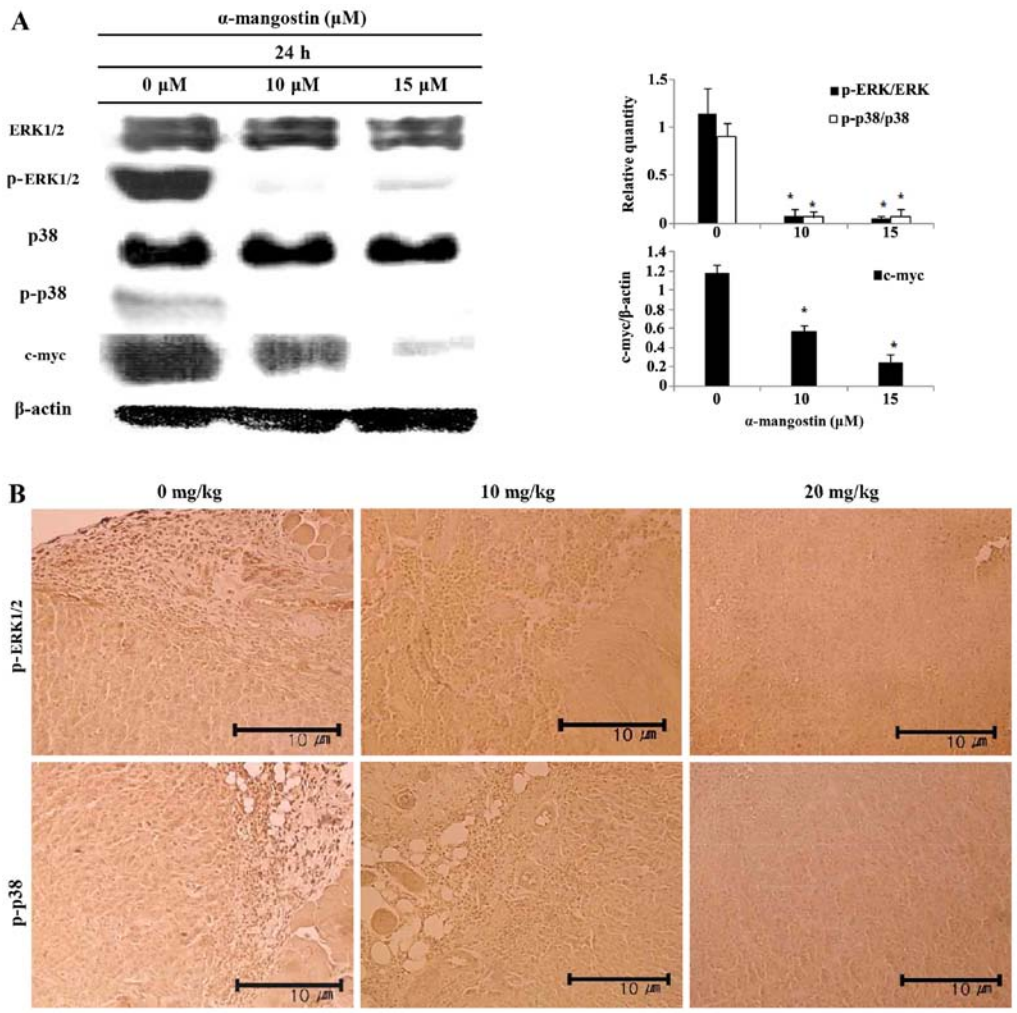

Figure 6. Effects of α-mangostin on extracellular signal-regulated kinase 1/2 (ERK1/2) and p38 signaling in YD-15 cells. (A) YD-15 cells were treated with α-mangostin (0, 10 and 15 μM) for 24 h. Cell lysates were prepared as described in the Material and methods and analyzed by 12% SDS-PAGE, followed by western blot analysis. The membranes were incubated with anti-ERK1/2, anti-p-ERK1/2, anti-p38, anti-p-p38, and anti-c-myc antibodies. Blots were also probed with the anti-β-actin antibody to confirm equal sample loading. (B) Nude mice were treated with α-mangostin (0, 10 and 20 mg/kg) for 22 days. To identify target proteins (p-ERK1/2, p-p38), immunohistochemistry was performed as described in the Material and methods. p-ERK1/2 and p-p38 were observed under a microscope and photographed (x200 magnification). Paraffin-embedded tumors were sectioned to 5-μm thickness.

mined to be 0.25, 0.08 and 0.05 g in the control, and 10 and 20 mg/kg α-mangostin-treated groups, respectively, indicating a decreasing trend in tumor weight upon the administration of α-mangostin (Fig. 7B). A TUNEL assay was performed on the extracted tumor tissue to examine cell apoptosis. As a result, many apoptotic cells were confirmed in the mice treated with α-mangostin compared with the control group (Fig. 7C). Immunohistochemical analysis was also performed to examine the expression of Ki-67, the protein responsible for the rate of tumor growth (Fig. 8). The tumor samples from the mice treated with α-mangostin exhibited a decreased Ki-67 expression in a concentration-dependent manner, suggesting that α-mangostin induced the apoptosis of YD-15 cells (in the tumor xenografts), thus inhibiting tumor growth.

Discussion

Surgical therapies, radiation therapies, medications and other current treatments for oral cancer are associated with a low treatment efficacy and severe adverse effects; thus, in general, oral cancer has a poor prognosis. Thus, it is important to develop a treatment strategy that selectively destroys cancer cells without inducing any toxic effects. In some studies, it was reported that several naturally derived substances induce apoptosis and inhibit cancer cell growth (21-24). α-mangostin, a naturally-derived substance, is extracted from the pericarp of the mangosteen fruit. α-mangostin was initially reported to be a substance that induces the apoptosis of cancer cells, particularly that of mammary, colorectal and liver cancer cells (16,18,19); however, the mechanisms responsible for the apoptosis induced by α-mangostin in oral cancer cells remain unknown.

In this study, an MTT assay was performed to confirm the inhibitory effects of α-mangostin on cell viability (Fig. 2A). The YD-15 cells treated with α-mangostin exhibited a concentration-dependent decrease in viability; at a concentration of 15 μM α-mangostin, there was an approximate inhibition rate of 58%. According to a previous study by Shibata *et al* (19), proliferation was significantly decreased in BJMC3879luc2 cells treated with 12 μM α-mangostin for 24 and 48 h. In another study by Hsieh *et al* (16), an inhibition rate of 50% was observed in

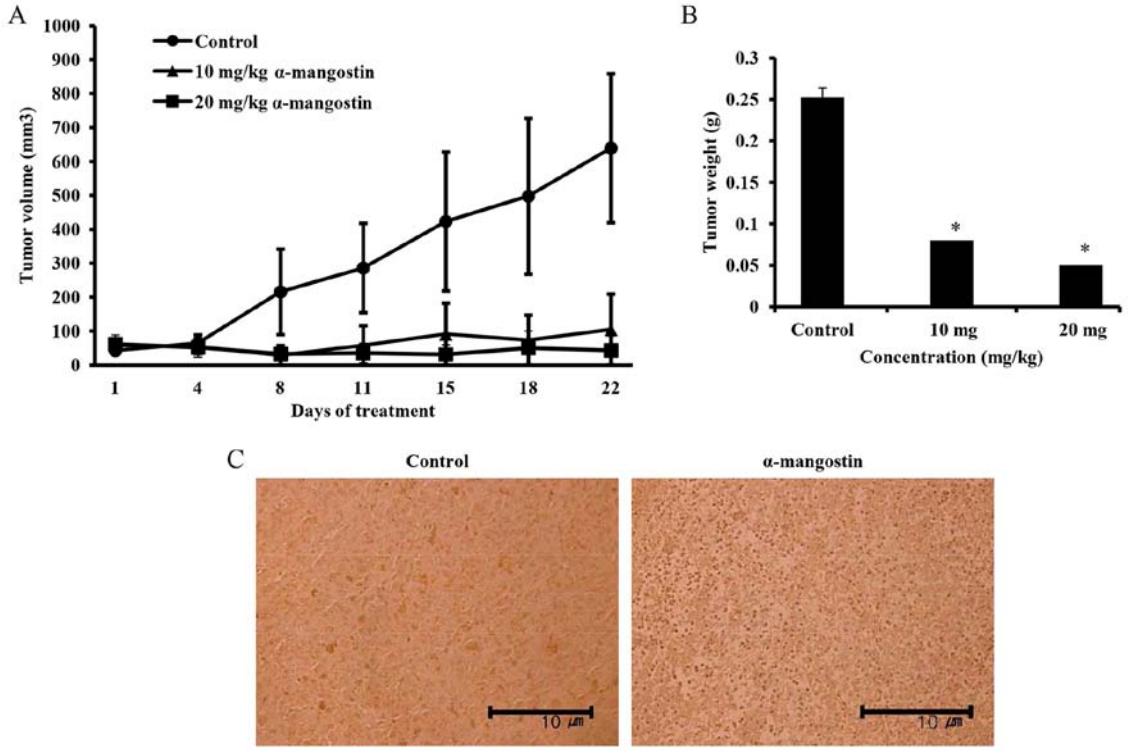

Figure 7. Inhibition of YD-15 oral cavity tumor growth and increased apoptosis upon treatment with α-mangostin. α-mangostin inhibits YD-15 xenograft growth in nude mice and induces apoptosis. Male BALB/c nude mice received an injection of YD-15 cells and were subsequently divided into 3 groups. α-mangostin was administered at a dose of 10 and 20 mg/kg 5 times per week for a total of 15 injections. On day 22, mice were sacrificed and tumors excised. (A) α-mangostin significantly reduced tumor volume from day 8 of treatment and onward. (B) Mean tumor weights in mice treated with α-mangostin were smaller than those in controls. Significance was determined by Dunnett's t-test. *P<0.05, significant difference compared with untreated controls. (C) Nude mice were treated with α-mangostin (0 and 10 mg/kg) for 22 days and analyzed by TUNEL assays.

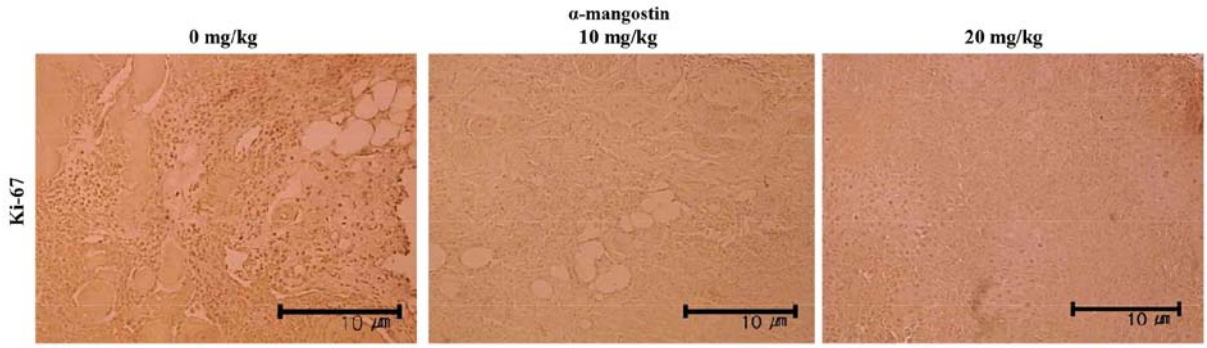

Figure 8. Effects of α-mangostin on Ki-67 expression. To identify Ki-67 protein expression, immunohistochemistry was performed as described in the Material and methods. Slides were observed under a microscope and photographed (x200 magnification). Paraffin-embedded tumors were sectioned to 5-μm thickness.

SK-Hep-1 cells treated with 24.8 μM α-mangostin for 24 h. The cells treated with 19.6 μM α-mangostin for 48 h also exhibited an inhibition rate of 50% (16). The findings of these other studies were similar to those from our study, in which α-mangostin decreased the viability of YD-15 tongue cancer cells in a concentration-dependent manner; therefore, α-mangostin is believed to effectively inhibit cancer cell proliferation.

Apoptosis, otherwise known as programmed cell death, is characterized by a number of well-defined features, such as condensation and fragmentation of chromatin, internucleosomal DNA cleavage, caspase activation and the translocation of phosphatidylserine from the inner to the outer leaflet of the plasma membrane (25). In the present study, these morphological changes were further examined by DAPI staining, in order to examine the inhibitory effects of α-mangostin on YD-15 cell viability. Based on DAPI staining, the number of apoptotic bodies in the cells treated with α-mangostin increased in a concentration-dependent manner compared to the control group (Fig. 2B). Thus, the distinct characteristics of apoptosis (i.e., shrinking of the cytoplasm, chromosomal condensation and apoptotic body formation) were observed.

The apoptotic cells were analyzed quantitatively by flow cytometry to determine whether the morphological changes observed in the DAPI-stained chromosomes were caused by apoptosis. In addition, the cell cycle was analyzed to examine the inhibitory effects of α-mangostin on cell cycle progression.

The apoptotic cells were first analyzed by Annexin V FITC/PI staining. The percentage of apoptotic cells was 16.06% in the control group and increased to 28.1 and 33.65% in the groups treated with 10 and 15 μM α-mangostin, respectively (Fig. 3A). Li *et al* (26) previously examined apoptotic MCF-7 and MDA-MB-231 cells treated with 0, 1, 2 and 4 μM α-mangostin for 24 h; they detected 4.19, 5.42, 8.89 and 27.96% apoptotic cells among the MCF-7 cells and 6.69, 7.97, 11.42 and 42.34% among the MDA-MB-231 cells, respectively. Moreover, the observed increases were concentration-dependent. Based on the findings of previous studies and those of our study, we concluded that α-mangostin induced cancer cell apoptosis in a concentration-dependent manner.

From the perspective of cell proliferation, cancer cells can be defined as being resistant to cell cycle control (27). Thus, as regards the development of particular anticancer drugs and preventive medications, the extent that a substance affects cancer cell cycle progression should be identified. In general, if apoptosis is induced *in vitro* and *in vivo*, an increase in the sub-G1 population is observed along with DNA fragmentation (28,29). In other words, an increase in the proportion of sub-G1 cells reflects an increase in apoptosis. In the present study, flow cytometry was used to analyze the cell cycle to examine the inhibitory effects of α-mangostin on different cell cycle phases. No significant differences were observed in the distribution of G1, S or G2/M cells, whereas the sub-G1 cell populations in the control group and groups treated with 10 and 15 μM α-mangostin were 0.28, 1.38 and 6.08%, respectively (Fig. 3B). Based on these results, we concluded that the inhibitory effects of α-mangostin on cell proliferation, particularly on the sub-G1 cell cycle arrest, were induced by apoptosis.

Apoptosis occurs via an organic reaction of various proteins controlled by internal/external cellular pathways. Bcl-2 family proteins control membrane permeability and are located in the mitochondrial membrane or move to the mitochondrial membrane to induce apoptotic cell death (30). Bax and Bad are pro-apoptotic factors that promote apoptosis, whereas Bcl-2 is an anti-apoptotic factor (31,32). In this study, the expression levels of Bax and Bcl-2 were measured by western blot analysis, which revealed that the expression of the pro-apoptotic factor, Bax, was increased and the expression of Bcl-2 was decreased in the α-mangostin-treated cells in a concentration-dependent manner (Fig. 4). This result implied that α-mangostin increased Bax expression in the YD-15 cells and decreased Bcl-2, ultimately leading to apoptosis.

Caspases are key factors that control apoptosis and are involved in a common pathway of various apoptotic signals. Caspases are further classified into initiator and effector caspases. Initiator caspases are activated by death signals to further activate the effector caspases (33). Caspase-3, which is activated by caspase-9, can cleave proteins involved in damaged DNA recovery or PARP. Caspase activation and PARP cleavage are typical characteristics of apoptosis (34). In this study, the levels of caspase-9 (initiator caspase), caspase-3 (effector caspase) and PARP were measured by western blot analysis in order to confirm the effects of α-mangostin on caspase activity in YD-15 cells. Both caspase-3 and -9 were activated, as evidenced by the increased levels of the respective cleaved forms, as well as PARP segmentation (Fig. 5A). The results of immunohistochemical analysis of cleaved caspase-3 were similar to those of western blot analysis (Fig. 5B). Considering these results, it appears that caspase plays a significant role in the apoptosis induced by α-mangostin in YD-15 tongue carcinoma cells, and the activation of caspase-9 and caspase-3 leads to PARP segmentation.

The MAPK signaling pathway is a core factor controlling various pathways, including cell growth, proliferation, segmentation and apoptosis. One of the key players in the MAPK pathway, ERK1/2, is activated by growth factors, such as those that promote apoptosis and further control cell growth, survival and division. Another key component of the MAPK pathway, p38 MAPK, is activated by chemical and environmental stresses and inflammatory factors that affect cellular levels (35). ERK1/2 and p38 activation through various pathways results in their translocation to the nucleus, where they function as transcription factors for early response proteins, such as c-myc and c-jun (36). Among the genes activated by the ERK1/2 signaling pathway, c-myc plays a major role in tumorigenesis (37). The c-myc protein level is strictly regulated by ERK1/2 through post-translational mechanisms (38). In this study, the levels of ERK1/2, p38 and c-myc were investigated by western blot analysis in order to verify the involvement of the ERK1/2 and p38 MAPK pathways in the apoptosis induced by α-mangostin. We determined that both ERK1/2 and p38 were deactivated via reduced phosphorylation. The expression of c-myc also decreased. Based on immunohistochemical analysis, the levels of p-ERK1/2 and p-p38 were found to decrease in a concentration-dependent manner (Fig. 6). According to a previous study, no significant differences were observed with respect to p-ERK1/2 and p-JNK1/2 activation in SK-Hep-1 cells treated with 10, 20 and 30 μM α-mangostin for 24 h, compared with the control group, whereas p-p38 decreased in a concentration-dependent manner (16). These results confirmed that the inhibition of p38 MAPK played a crucial role in apoptosis induced by α-mangostin in cancer cells (16). Moreover, in another study, no significant changes were observed in SW1353 cells treated with 20 μg/ml α-mangostin for 0, 3 and 6 h with respect to p-p38 activation, whereas p-ERK1/2 tended to increase after 3 h and decrease after 6 h, along with p-JNK. Thus, the inhibition of p-ERK1/2 was associated with the apoptosis induced by α-mangostin (39). Taking into consideration the findings of previous studies, as well as those from our study, we hypothesized that α-mangostin inhibited the activation of ERK1/2 and p38 MAPK signaling pathways, which further inhibited the expression of the c-myc oncogene.

In this study, YD-15 cells were also administered to nude mice to confirm the *in vivo* anticancer efficacy of α-mangostin. Mice were divided into 3 groups: the control (vehicle-treated) and the 10 and 20 mg/kg α-mangostin treatment groups. α-mangostin was administered intraperitoneally 5 times/week. A marked difference between the treated and control groups was observed beginning on day 8 following treatment (Fig. 7A). On day 22, tumors in the 20 mg/kg α-mangostin treatment group exhibited an inhibition rate of 89.9%. A TUNEL assay was performed on tumors extracted from the experimental nude mice, which revealed a significant increase in the expression of TUNEL-positive cells in the α-mangostin-treated group (Fig. 7C).

A Ki-67 antibody was used to differentiate nuclei in proliferating cells (G1, S, G2 and M phases) from those in resting cells, as previously described (40). Immunohistochemical analysis

confirmed the expression of Ki-67, a protein used to determine the rate of proliferation of cancer cells, and demonstrated that its expression was decreased in the α-mangostin-treated mice (Fig. 8). According to these results, α-mangostin induced the apoptosis of YD-15 cells and inhibited cell proliferation.

In conclusion, in the present study, we demonstrated that treatment with α-mangostin leads to cellular apoptosis through the inhibition of ERK1/2 and p38 MAPK signaling in YD-15 tongue carcinoma cells, indicating the potential use of of α-mangostin as an anticancer treatment, particularly for the treatment of oral cancer.

Acknowledgements

This study was supported by a research grant of the Kongju National University in 2014.

References

1. Jung KW, Won YJ, Kong HJ, Oh CM, Cho HS, Lee DH and Lee KH: Cancer statistics in Korea: incidence, mortality, survival, and prevalence in 2012. Cancer Res Treat 47: 127-141, 2015.
2. Neville BW and Day TA: Oral cancer and precancerous lesions. CA Cancer J Clin 52: 195-215, 2002.
3. Silverman S: Early diagnosis of oral cancer. Cancer 62: 1796-1799, 1998.
4. Kim MY, Kim CS, Lee SH, Kim JW and Jang HJ: A clinicostatistical analysis of oral cancer patients for recent 8 years. J Korean Assoc Oral Maxillofac Surg 33: 660-668, 2007.
5. Lee EJ, Kim MJ and Myoung H: Change of the invasiveness with selective Cox-2 inhibition in an oral squamous cell carcinoma cell Line, KB: preliminary in vitro study. J Korean Assoc Oral Maxillofac Surg 33: 103-108, 2007.
6. Mahabusarakam W, Wiriyachitra P and Taylor WC: Chemical constituents of *Garcinia mangostana*. J Nat Prod 50: 474-478, 1987.
7. Jung HA, Su BN, Keller WJ, Mehta RG and Kinghorn AD: Antioxidant xanthones from the pericarp of *Garcinia mangostana* (Mangosteen). J Agric Food Chem 54: 2077-2082, 2006.
8. Akao Y, Nakagawa Y, Iinuma M and Nozawa Y: Anti-cancer effects of xanthones from pericarps of mangosteen. Int J Mol Sci 9: 355-370, 2008.
9. Iinuma M, Tosa H, Tanaka T, Asai F, Kobayashi Y, Shimano R and Miyauchi K: Antibacterial activity of xanthones from guttiferaeous plants against methicillin-resistant *Staphylococcus aureus*. J Pharm Pharmacol 48: 861-865, 1996.
10. Sundaram BM, Gopalakrishnan C, Subramanian S, Shankaranarayanan D and Kameswaran L: Antimicrobial activities of *Garcinia mangostana*. Planta Med 48: 59-60, 1983.
11. Chen LG, Yang LL and Wang CC: Anti-inflammatory activity of mangostins from *Garcinia mangostana*. Food Chem Toxicol 46: 688-693, 2008.
12. Shan T, Ma Q, Guo K, Liu J, Li W, Wang F and Wu E: Xanthones from mangosteen extracts as natural chemopreventive agents: potential anticancer drugs. Curr Mol Med 11: 666-677, 2011.
13. Jiang DJ, Dai Z and Li YJ: Pharmacological effects of xanthones as cardiovascular protective agents. Cardiovasc Drug Rev 22: 91-102, 2004.
14. Nakatani K, Yamakuni T, Kondo N, Arakawa T, Oosawa K, Shimura S, Inoue H and Ohizumi Y: γ-Mangostin inhibits inhibitor-kappaB kinase activity and decreases lipopolysaccharide-induced cyclooxygenase-2 gene expression in C6 rat glioma cells. Mol Pharmacol 66: 667-674, 2004.
15. Pedraza-Chaverri J, Cárdenas-Rodríguez N, Orozco-Ibarra M and Pérez-Rojas JM: Medicinal properties of mangosteen (*Garcinia mangostana*). Food Chem Toxicol 46: 3227-3239, 2008.
16. Hsieh SC, Huang MH, Cheng CW, Hung JH, Yang SF and Hsieh YH: α-Mangostin induces mitochondrial dependent apoptosis in human hepatoma SK-Hep-1 cells through inhibition of p38 MAPK pathway. Apoptosis 18: 1548-1560, 2013.
17. Johnson JJ, Petiwala SM, Syed DN, Rasmussen JT, Adhami VM, Siddiqui IA, Kohl AM and Mukhtar H: α-Mangostin, a xanthone from mangosteen fruit, promotes cell cycle arrest in prostate cancer and decreases xenograft tumor growth. Carcinogenesis 33: 413-419, 2012.
18. Watanapokasin R, Jarinthanan F, Nakamura Y, Sawasjirakij N, Jaratrungtawee A and Suksamrarn S: Effects of α-mangostin on apoptosis induction of human colon cancer. World J Gastroenterol 17: 2086-2095, 2011.
19. Shibata MA, Iinuma M, Morimoto J, Kurose H, Akamatsu K, Okuno Y, Akao Y and Otsuki Y: α-Mangostin extracted from the pericarp of the mangosteen (*Garcinia mangostana* Linn) reduces tumor growth and lymph node metastasis in an immunocompetent xenograft model of metastatic mammary cancer carrying a p53 mutation. BMC Med 9: 69, 2011.
20. Xia Z, Dickens M, Raingeaud J, Davis RJ and Greenberg ME: Opposing effects of ERK and JNK-p38 MAP kinases on apoptosis. Science 270: 1326-1331, 1995.
21. Surh YJ, Hurh YJ, Kang JY, Lee E, Kong G and Lee SJ: Resveratrol, an antioxidant present in red wine, induces apoptosis in human promyelocytic leukemia (HL-60) cells. Cancer Lett 140: 1-10, 1999.
22. Aisa Y, Miyakawa Y, Nakazato T, Shibata H, Saito K, Ikeda Y and Kizaki M: Fucoidan induces apoptosis of human HS-sultan cells accompanied by activation of caspase-3 and down-regulation of ERK pathways. Am J Hematol 78: 7-14, 2005.
23. Lazzè MC, Savio M, Pizzala R, Cazzalini O, Perucca P, Scovassi AI, Stivala LA and Bianchi L: Anthocyanins induce cell cycle perturbations and apoptosis in different human cell lines. Carcinogenesis 25: 1427-1433, 2004.
24. Shim HY, Park JH, Paik HD, Nah SY, Kim DSHL and Han YS: Acacetin-induced apoptosis of human breast cancer MCF-7 cells involves caspase cascade, mitochondria-mediated death signaling and SAPK/JNK1/2-c-Jun activation. Mol Cells 24: 95-104, 2007.
25. Talib WH and Mahasneh AM: Antiproliferative activity of plant extracts used against cancer in traditional medicine. Sci Pharm 78: 33-45, 2010.
26. Li P, Tian W and Ma X: Alpha-mangostin inhibits intracellular fatty acid synthase and induces apoptosis in breast cancer cells. Mol Cancer 13: 138, 2014.
27. Evan GI and Vousden KH: Proliferation, cell cycle and apoptosis in cancer. Nature 411: 342-348, 2001.
28. Korystov YN, Mosin VA, Shaposhnikova VV, Levitman MK, Kudryavtsev AA, Kruglyak EB, Sterlina TS, Vik-torov AV, Drinyaev VA: A comparative study of effects of aversectin C abamectin and ivermectin on apoptosis of rat thymo-cytes induced by radiation and dexamethasone. Acta Vet Brno 68: 23-29, 1999.
29. Badran A, Iwasaki H, Inoue H and Ueda T: Atypical nuclear apoptosis downstream to caspase-3 activation in ara-C treated CCRF-CEM cells. Int J Oncol 22: 517-522, 2003.
30. Willis S, Day CL, Hinds MG and Huang DC: The Bcl-2-regulated apoptotic pathway. J Cell Sci 116: 4053-4056, 2003.
31. Chiarugi V, Magnelli L, Cinelli M and Basi G: Apoptosis and the cell cycle. Cell Mol Biol Res 40: 603-612, 1994.
32. Donovan M and Cotter TG: Control of mitochondrial integrity by Bcl-2 family members and caspase-independent cell death. Biochim Biophys Acta 1644: 133-147, 2004.
33. Bao Q and Shi Y: Apoptosome: a platform for the activation of initiator caspases. Cell Death Differ 14: 56-65, 2007.
34. Galluzzi L, Kepp O, Trojel-Hansen C and Kroemer G: Mitochondrial control of cellular life, stress, and death. Circ Res 111: 1198-1207, 2012.
35. Chuang SM, Wang IC and Yang JL: Roles of JNK, p38 and ERK mitogen-activated protein kinases in the growth inhibition and apoptosis induced by cadmium. Carcinogenesis 21: 1423-1432, 2000.
36. Bassi R, Heads R, Marber MS and Clark JE: Targeting p38-MAPK in the ischaemic heart: kill or cure? Curr Opin Pharmacol 8: 141-146, 2008.
37. Hatano K, Yamaguchi S, Nimura K, Murakami K, Nagahara A, Fujita K, Uemura M, Nakai Y, Tsuchiya M, Nakayama M, *et al*: Residual prostate cancer cells after docetaxel therapy increase the tumorigenic potential via constitutive signaling of CXCR4, ERK1/2 and c-Myc. Mol Cancer Res 11: 1088-1100, 2013.
38. Sears R, Nuckolls F, Haura E, Taya Y, Tamai K and Nevins JR: Multiple Ras-dependent phosphorylation pathways regulate Myc protein stability. Genes Dev 14: 2501-2514, 2000.
39. Krajarng A, Nakamura Y, Suksamrarn S and Watanapokasin R: α-Mangostin induces apoptosis in human chondrosarcoma cells through downregulation of ERK/JNK and Akt signaling pathway. J Agric Food Chem 59: 5746-5754, 2011.
40. Gerdes J, Lemke H, Baisch H, Wacker HH, Schwab U and Stein H: Cell cycle analysis of a cell proliferation-associated human nuclear antigen defined by the monoclonal antibody Ki-67. J Immunol 133: 1710-1715, 1984.